Structural Characterization of Soluble Lignin in the Pre-Hydrolysis Liquor of Bamboo-willow Dissolving Pulp

Jinchao Zhang,[a] Chaojun Wu,[a,b,*] Dongmei Yu,[a] and Yachong Zhu [a]

The soluble lignin present in the pre-hydrolysis liquor (PHL) is detrimental for value-added utilization of the PHL from production of kraft-based dissolving pulp. In this paper, the soluble lignin was separated from PHL by activated carbon adsorption and subsequent desorption with methanol. The structural characteristics of the soluble and dioxane lignins (from bamboo-willow material) were analyzed by Fourier transform infrared (FTIR) spectroscopy, nuclear magnetic resonance (NMR), and thermogravimetric analysis (TGA). The FTIR and proton-NMR results showed that cleavage of *β*-O-4 aryl-ether linkages and demethylation occurred in the lignin structure during the pre-hydrolysis. The main linkages between structural monomeric units of the soluble lignin were *β*-*β*, *β*-5, *β*-1, and *β*-O-4. Additionally, the TGA results showed that the residual char yield at 800 °C of the soluble and dioxane lignins were 33.4% and 35.3%, respectively. Therefore, the soluble lignin obtained from PHL possessed thermal stability comparable to that of dioxane lignin, and can be used as a renewable source for carbon fiber.

Keywords: Dissolving pulp; Pre-hydrolysis liquor; Soluble lignin; Structural characteristics

Contact information: a: State Key Laboratory of Biobased Material and Green Papermaking, Qilu University of Technology, Shandong Academy of Sciences, Jinan, 250353; b: State Key Laboratory of Pulp and Paper Engineering, South China University of Technology, Guangzhou, 510640;
**Corresponding author: chaojunwu2007@163.com*

INTRODUCTION

Pre-hydrolysis liquor (PHL) is considered a waste liquor produced in the first step of the kraft-based dissolving pulp production process. The PHL contains a substantial amount of degradation products derived from lignocellulosic materials, such as saccharides formed from hemicelluloses, lignin derivatives, and acetic acid. The saccharides present in the PHL can be further processed to produce biofuels, biochemicals, functional oligosaccharides, *etc*. (Kumar and Christopher 2017). The lignin present in the PHL can be used to produce biofuel, plastics, phenols, *etc*. (Schorr *et al*. 2014). However, the presence of lignin in the PHL is detrimental for value-added utilization of saccharides. Lignin adversely affects the fermentation of xylose/xylan in the PHL into ethanol or xylitol (Lee *et al*. 2013). In addition, the presence of lignin in the PHL may hinder the separation and concentration of acetic acid (Yang *et al*. 2013a). Therefore, the removal of soluble lignin from the PHL is essential for the further resource utilization of the PHL. Such as approach not only conforms to the forest biorefinery concept, but also can add additional revenue to the dissolving pulp industry.

In the pre-hydrolysis stage, the lignin macromolecules are depolymerized and degraded under high temperature and acidic reaction conditions. During this step, the main *β*-O-4 aryl ether linkages in lignin undergo homolytic cleavage, resulting in an increase in the content of free phenolic hydroxyl groups (Evtuguin *et al*. 2001).

After depolymerization, the lignin is converted into oligomers, dimers, and monomers rich in phenolic hydroxyl groups (Bardet *et al*. 1985). As the pre-hydrolysis step proceeds, the lignin moieties further undergo repolymerization or condensation reactions as shown by the increase in the contents of -C-C- bonds and the decrease of β-O-4 linkages (Capanema *et al*. 2005). Chua and Wayman (1979) studied the hot water pre-hydrolysis of poplar wood and observed the formation of lignin condensation products, which was attributed to a series of reactions occurring between lignin aromatic rings, furfural, and hydroxymethyl-furfural. Under strong acidic conditions, the diphenylmethane structure is the main product of the lignin condensation reaction. During the pre-hydrolysis, a stilbene structure also can be formed from the *β*-1 structure and the cleavage of *β*-O-4 bonds (Leschinsky *et al*. 2008). Mašura (1987) showed that lignin would be re-deposited in the later stage of pre-hydrolysis, causing re-adsorption to the surface of wood chips. The condensation and re-deposition of lignin during the pre-hydrolysis process will impart adverse effects on subsequent cooking and bleaching.

The structural characteristics of soluble lignin in the PHL have a great influence on its specific removal. Therefore, it is important to study the structure and properties of soluble lignin in the PHL for the selective removal of soluble lignin. Various investigations have been conducted on separation and structural characterization of lignin in the PHL. Yang *et al*. (2013b) separated lignin from the PHL *via* acidification, and characterized its structure. Results showed that PHL lignin has a lower methoxyl content and molecular weight compared to dioxane lignins. Chen *et al*. (2019) studied the structure of lignin after separating lignin from PHL by hydrothermal acid hydrolysis, the results showed that the lignin samples obtained revealed relatively high molecular weight, surface hydrophilicity, and thermal stability. Tong *et al*. (2017) studied the structure of lignin in the PHL *via* acidification treatment (AT) and rotary vacuum evaporation treatment (RVET), and the results showed that the RVET lignin could be identified as *p*-hydroxyphenyl (H), syringyl (S), guaiacyl (G) lignins, and the AT lignin was mainly composed of S-lignin that had *β*-1, *β*-5, *β*-O-4, and *β*-*β* bonds. Wang *et al*. (2014a) separated lignin samples from the PHL by activated carbon adsorption, and studied the effect of laccase treatment on the molecular weight of lignin in the PHL.

However, the structure of soluble lignin in PHL has not been clearly studied. To enhance the removal of soluble lignin from PHL, the structural characteristic of soluble lignin should be further explored. The study of Wang *et al*. (2014b) demonstrated that phenolic hydroxyl groups (PhOH) in lignin played an important role in the removal lignin from PHL.

In the present study, the PHL of bamboo-willow dissolving pulp was prepared by using the optimized parameters in our previous research (Zhang *et al*. 2019). The soluble lignin was separated from PHL *via* activated carbon adsorption and subsequent desorption using methanol, and then the soluble lignin samples thus obtained were purified. For comparison, the dioxane lignin was also prepared and separated from the bamboo-willow material. The isolated lignin samples were characterized by Fourier transform infrared (FTIR), proton nuclear magnetic resonance (^{1}H-NMR), two dimensional heteronuclear single quantum correlation (2D-HSQC) spectroscopies, and thermogravimetric analysis (TGA).

EXPERIMENTAL

Materials

The raw material of bamboo-willow (*Salix* sp or zhuliu in Chinese) was provided by one of the forestry centers in the Xinjiang autonomous region of Wulumuqi, China. The chemical compositional analysis of the raw material revealed 77.2% holocellulose, 40.4% α-cellulose, 24.1% pentosan, 20.3% acid-insoluble lignin, and 3.46% acid-soluble lignin (Zhang *et al*. 2019). Chipped bamboo-willow was screened to obtain particles with the dimensions of 15 mm to 20 mm (length) × 10 mm to 20 mm (width) × 3 mm to 5 mm (thickness). A portion of the wood chips was taken for moisture content determination for subsequent experiments.

Methods

Preparation of PHL

Pre-hydrolysis was performed in an electrically heated stainless-steel digester (15-L) with 1.0 kg oven-dried chips at a reaction temperature of 160 °C for 90 min (Zhang *et al*. 2019). Deionized water was added to reach a 6:1 liquid-to-wood ratio. The dosage of phosphoric acid used was 0.5% (based on the oven-dried weight of the materials). Upon completion of pre-hydrolysis, the digester was cooled by decompressing the exhaust valve, which subsequently separated the PHL from the solid mass. The collected PHL was slowly filtered using two-tiers of quantitative filter papers and then refrigerated for experimental use. The contents of soluble lignin, arabinose, galactose, glucose, xylose, mannose, and total sugars in original PHL were 4.84, 0.91, 1.00, 4.02, 8.67, 1.17, and 15.8 g/L, respectively.

Analytical methods

The soluble lignin content in the PHL was measured *via* ultraviolet visible (UV-vis) spectroscopy (Agilent 8453; Agilent Technologies Inc., Palo Alto, CA, USA) at a wavelength of 205 nm, according to TAPPI um 250 (2000) (Wang *et al*. 2014a).

The sugars content in the PHL was measured using an indirect method based on quantitative acid hydrolysis of the liquid sample. To convert the oligomeric sugars in the PHL to monomeric sugars, the PHL was acid hydrolyzed using 4 wt% sulfuric acid at 121 °C for 1 h in an oil bath according to a technical report from the National Renewable Energy Laboratory (NREL) (Sluiter *et al*. 2006; Shen *et al*. 2011). The acid-hydrolyzed PHL was then diluted, and the content of monomeric sugars was measured. The monomeric sugars were measured using high-performance anion-exchange chromatography coupled with a pulsed amperometric detector (HPAEC-PAD) and an HPAEC-PAD system (ICS-5000; Thermo Fisher Scientific, Sunnyvale, CA, USA) equipped with a CarboPac PA20 analytical column (3 mm × 150 mm) (Thermo Fisher Scientific, Sunnyvale, CA, USA) and guard column (3 mm × 30 mm). The samples were filtered through 0.22-μm syringe filters prior to injection. The concentration of the sugars after this additional hydrolysis stage reflected the total sugars content of the PHL (Shen *et al*. 2011).

Lignin isolation from PHL

The method of separating lignin from the PHL was achieved by following the method of Shen *et al*. (2013) and Wang *et al*. (2014a). The mixture of PHL and activated carbon at a ratio of 30:1 (m/m) was shaken at 250 rpm at room temperature for 5 h. Then, the mixture was filtered with Whatman (Q8) filter paper and air-dried at room temperature

for 48 h. The air-dried lignin/activated carbon mixture was then mixed with methanol at a ratio of 30:1 at room temperature for 5 h at 250 rpm for three replicates. Finally, the lignin sample was obtained by filtration followed by vacuum rotary evaporation (IKA, Staufen, Germany), and dried in a vacuum oven with P_2O_5 at 50 °C.

Lignin isolation from raw material

The wood meal of 40/60-mesh was extracted with benzene-ethanol for 8 h, and vacuum-dried over P_2O_5. The extracted wood meals were extracted with an acidic aqueous dioxane (90% v/v) solution for 1 h, in N_2 atmosphere. The HCl concentration in the dioxane solution was 0.2 mol/L. The dioxane solution-to-wood meal ratio was kept at 8:1. Upon completion of refluxing, the mixture was filtered with a Buchner funnel, and the residue was washed with an aqueous dioxane solution (90% v/v). The filtrate was neutralized with solid Na_2CO_3, and then the filtrate was collected by filtration. The filtrate was concentrated in a rotary vacuum evaporator at 40 °C, and the concentrated filtrate was slowly dropped into deionized water to precipitate lignin, the lignin precipitate was washed, and vacuum-dried with P_2O_5.

Lignin purification

Lignin purification was achieved by following the method of Yang *et al*. (2013b). The crude lignin separated from PHL and raw material were dissolved in dioxane solution (90% v/v), and precipitated in ether by magnetic stirrer. The precipitated lignin was vacuum-dried with P_2O_5.

Analysis Methods

FTIR analysis

The FTIR spectra of the samples were recorded with an IR-Prestige-21 spectrometer (Shimadzu, Kyoto, Japan). The dried lignin samples were embedded in KBr pellets at concentrations of approximately 1 mg/100 mg KBr. The spectra was recorded in the absorption mode in the 4000 cm^{-1} to 400 cm^{-1} range.

^{1}H-NMR analysis

The ^{1}H-NMR spectra of the samples were recorded on an AVANCE II 400 MHz NMR spectrometer (Bruker, Karlsruhe, Germany). Samples of approximately 30 mg were completely dissolved in 0.6 mL of dimethyl sulphoxide (DMSO-d6, 99.99%; Cambridge Isotope Laboratories, Andover, MA, USA). The chemical shifts were calibrated relative to the signals of DMSO solvent, which was used as an internal standard at 2.49 ppm for the ^{1}H-NMR spectra. The acquiring time (AQ) was 3.98 s, and the relaxation time used was 1.0 s.

2D-HSQC analysis

The 2D-HSQC analysis of the samples were recorded on an AVANCE II 400 MHz NMR spectrometer (Bruker, Karlsruhe, Germany). Samples of approximately 40 mg was dissolved in 0.6 mL of DMSO-d6 was used for NMR measurement.

TGA

The thermal stability of the samples was measured using a Q50 thermogravimetric analyzer (TA Instruments, New Castle DE, USA). Approximately 3.0 mg of sample was

heated from room temperature to 800 °C at a heating rate of 10 °C/min under N_2 atmosphere.

RESULTS AND DISCUSSION

FTIR Spectroscopy

The FTIR spectra of both the soluble and dioxane lignins were recorded, and are shown in Fig. 1. The peak assignments are presented in Table 1 following previous studies (Jahan and Mun 2007; Zhao *et al*. 2014; Constant *et al*. 2015). The absorption peaks at 1515 cm^{-1} and 1605 cm^{-1} were assigned to the skeletal vibrations of the benzene ring (aromatic units) and were selected as qualitative absorption of lignin (Buta *et al*. 1989; Kang *et al*. 2012). The absorption peaks at approximately 3410 cm^{-1} and 3460 cm^{-1} were assigned to the stretching of O-H groups, inclusive of alcoholic and phenolic hydroxyl groups (Yang *et al*. 2013b).

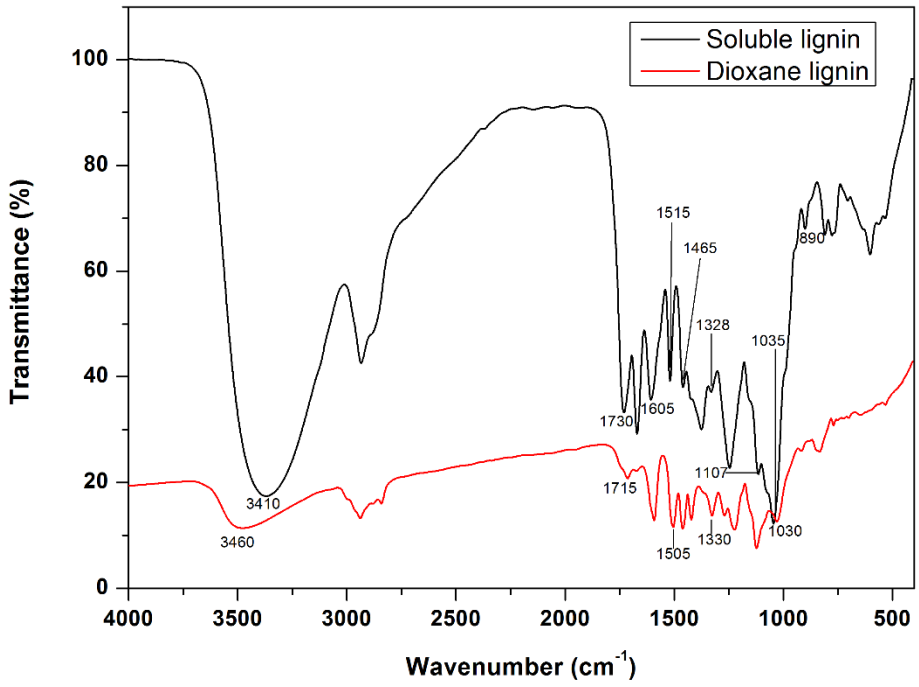

Fig. 1. FTIR spectra of soluble and dioxane lignins

The absorbance peak at 890 cm^{-1} was assigned to isolated aromatic C-H bond vibrations (Lora and Wayman 1980), which indicated that there was a condensation structure in the soluble lignin obtained from PHL. The band at 1505 cm^{-1} was shifted to 1515 cm^{-1} in soluble lignin fraction, which was probably caused by the decreased amount of *β*-O-4 linkages (Yang *et al*. 2013b). The band at 1325 cm^{-1} to 1330 cm^{-1} was related to the syringyl (S-type) structural unit of lignin, and the band at 1030 cm^{-1} to 1035 cm^{-1} belongs to the C-H bending of guaiacyl (G-type) structural units. These results indicated that there were mainly syringyl (S-type) and guaiacyl (G-type) structural units in both soluble (1328 cm^{-1} and 1035 cm^{-1}) and dioxane (1330 cm^{-1} and 1030 cm^{-1}) lignin fractions. A C=O structure in an unconjugated ketone group (*β*-carbonyl group) was observed at 1730

cm^{-1} (soluble lignin) and 1715 cm^{-1} (dioxane lignin). In addition, the band at 1465 cm^{-1} indicated C-H deformation and aromatic vibration. Further, the infrared spectra of the obtained soluble lignin showed that there was a weak absorbance peak at 1107 cm^{-1}. The band at 1107 cm^{-1} denoted the C-O vibration in carbohydrates (Tong *et al*. 2017), indicating that the soluble lignin obtained by activated carbon adsorption from PHL contained carbohydrates component.

Table 1. Assignments of FTIR Spectra of Soluble and Dioxane Lignins

Wavenumber (cm^{-1})	Assignments	Soluble Lignin	Dioxane Lignin
3400 to 3460	O-H Stretching	3410	3460
2842 to 3000	C-H Stretch in methyl and methylene groups	2940, 2880	2940
1709 to 1738	C=O Stretch in unconjugated ketone, carbonyl, and ester groups	1730	1715
1655 to 1675	C=O Stretching in conjugated *p*-substituted aryl ketones	1670	1675
1593 to 1605	Aromatic skeleton vibrations plus C=O stretching; S > G: $G_{condensed}$ > $G_{etherified}$	1605	1594
1505 to 1515	Aromatic skeleton vibrations (G > S)	1515	1505
1460 to 1470	C-H Deformations (asymmetrical in $-CH_3$ and $-CH_2-$)	1465	1462
1422 to 1430	Aromatic skeletal vibrations combined with C-H in plane deformations	1425	1422
1365 to 1370	Aliphatic C-H stretching in $-CH_3$ and phenolic -OH groups	1370	1370
1325 to 1330	Condensed S and G rings (G ring bound *via* position 5), syringyl unit	1328	1330
1266 to 1270	G Ring plus C + O stretching, guaiacyl unit	-	1270
1245	-	1245	-
1221 to 1230	C-C + C-O + C=O Stretchings ($G_{condensed}$ > $G_{etherified}$)	-	1221
1166	Typical for HGS lignins; C=O in ester groups (conjugated)	1166	1166
1140	Aromatic C-H in plane deformation (typical of G unit; $G_{condensed}$> Getherified）	-	-
1125 to 1128	Typical of S unit; also secondary alcohol and C=O stretching	-	-
1107	C-O Vibration in carbohydrate	1107	-
1085	C-O Deformation in secondary. alcohol and aliphatic ether	-	-
1030 to 1035	Aromatic C-H in plane deformation (G > S) plus C-O deformation in primary alcohols plus C-H stretching (unconjugated)	1035	1030
966 to 990	-C=C- Out of plane deformation (*trans*)	-	-
915 to 925	C-H Out of plane (aromatic ring)	-	920
853 to 858	C-H Out of plane in positions 2, 5, and 6 (G-units)	-	-
834 to 835	C-H Out of plane in positions 2 and 6 of S-units	-	-
817 to 832	C-H Out of plane in positions 2, 5, and 6 of G-units	-	-

^{1}H-NMR Analysis

The integrated ^{1}H-NMR spectra for the soluble and dioxane lignins are shown in Fig. 2. Table 2 lists the positions of signals assigned from previous reports (Jahan and Mun 2007; Kang and Zhou 2012; Yang *et al*. 2013b). In combination with the above FTIR analysis and the ^{1}H-NMR signals of the *p*-hydroxyphenyl aromatic protons (δ 7.48 ppm and 7.49 ppm), the soluble lignin from PHL could be justified as HSG lignin. According to Table 2, the phenolic hydroxyl (Ar-OH) content of the soluble lignin was lower than that of dioxane lignin, which indicated that the rupture of aryl-ether bond occurred during pre-hydrolysis (Jahan *et al*. 2012; Yang *et al*. 2013b).

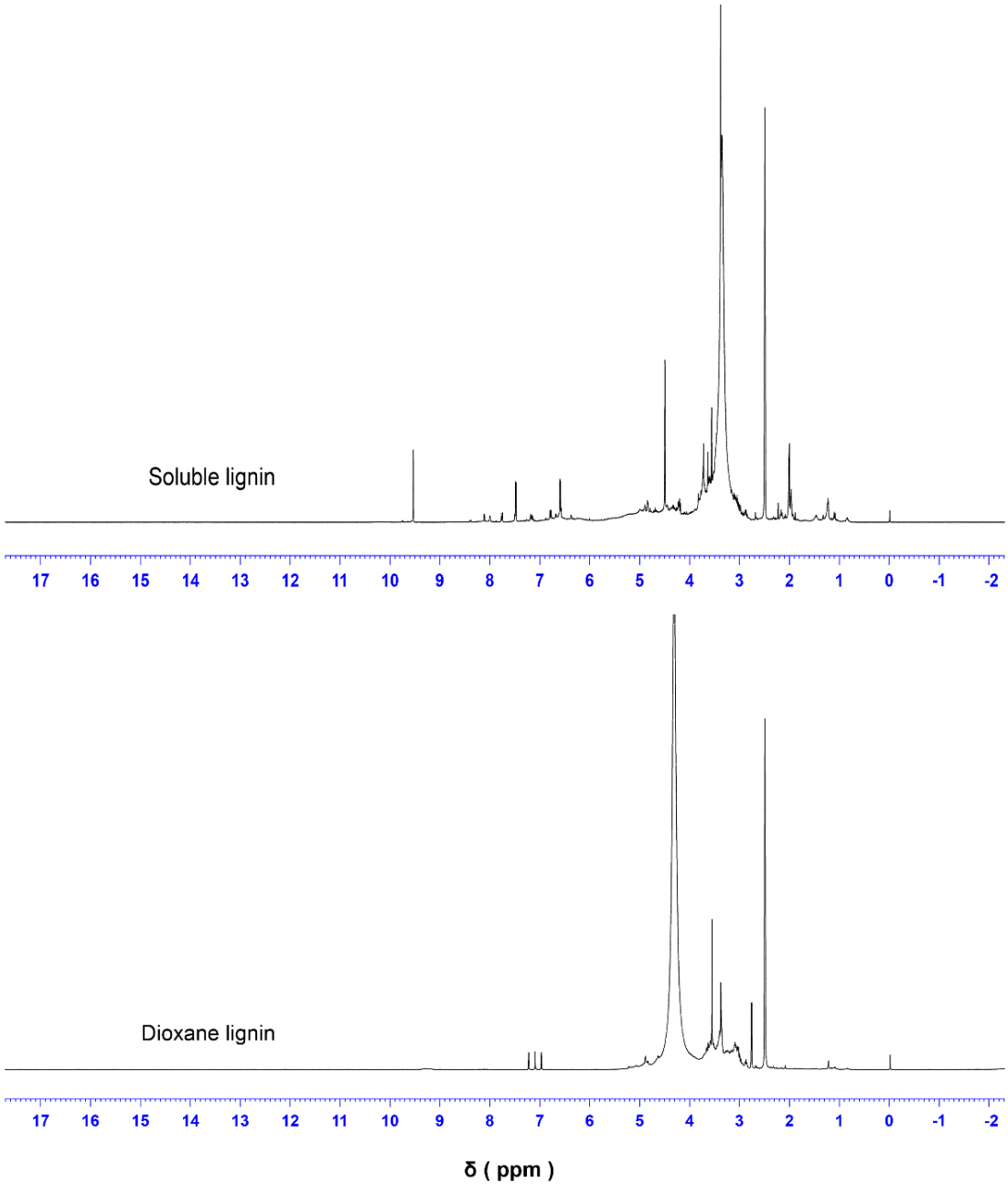

Fig. 2. ^{1}H-NMR spectra of the soluble and dioxane lignins

It is noteworthy that both soluble and dioxane lignins possessed absorbance peaks at the range of δ 3.00 ppm to 4.15 ppm (methoxyl groups). Further, the methoxyl content of soluble lignin was lower than that of dioxane lignin, indicating the demethylation of the aromatic methoxyl groups in the lignin structure occurred during pre-hydrolysis, this was consistent with the results of Ibrahim *et al.* (2010). In addition to this observation, the peak strength at 2.49 ppm was also strong, which denotes the absorbance peak for solvent DMSO-d6 (Tong 2017). The absorbance peaks at δ 1.23 ppm and 1.24 ppm correspond to the hydrogen atom in aliphatic groups, which may be caused by carbohydrates. Additionally, the cinnamyl alcohol structure was detected in both soluble (δ 4.34 ppm to 4.84 ppm) and dioxane (δ 4.31 ppm to 4.91 ppm) lignins.

Table 2. Assignments of Signals in the ^{1}H-NMR Spectra of Soluble and Dioxane Lignins

Range δ (ppm)	Assignments	Soluble Lignin	Dioxane Lignin
0.38 to 1.58	High-shadowing aliphatic proton	1.23, 1.24	1.22
1.58 to 2.19	H of aliphatic acetates	1.96, 1.97, 2.00, 2.01	-
2.19 to 2.50	H of aromatic acetates	2.23, 2.49	2.49
2.50 to 3.00	H_β of *β*-1, *β*-5, and *β*-*β* structures	2.98	2.76 to 3.00
3.00 to 4.15	H of methoxyl groups	3.01 to 3.83	3.00 to 4.00
4.15 to 4.30	H_γ of *β*-1, *β*-5, *β*-O-4, and *β*-*β* structures	4.19, 4.20, 4.21, 4.23	-
4.30 to 5.18	H*α* of *β*-*β* structure, H_β of *β*-O-4 structure, and H_γ of cinnamyl alcohol structure	4.34 to 4.84	4.31 to 4.91
6.28 to 6.80	Aromatic proton in syringyl units	6.59 to 6.60	-
7.30 to 7.80	Aromatic proton in *p*-hydroxyphenyl units	7.48, 7.49	-
8.00 to 11.5	Protons in carboxyl and aldehyde groups	9.54	-

2D-HSQC Analysis

To further understand the structural characteristics of the soluble lignin obtained from PHL, qualitative 2D-HSQC spectra of the soluble and dioxane lignins were recorded and are shown in Fig. 3, and the detailed peak assignments are presented in Table 3 (Del Rio *et al*. 2009; Xiao *et al*. 2012; Chen *et al*. 2019). The structure of the soluble lignin obtained from PHL can be analyzed more intuitively by combining the structure diagrams of several dimers, such as *β*-ether (*β*-O-4, A), and H, S, G-monomers of lignin as shown in Fig. 3 (Xiao *et al*. 2012).

In the side-chain region, the signal of C-H in methoxy group in the spectrum showed a strong correlation signal at δC/δH 56.0/3.7 ppm. The signals at δC/δH 63.5/4.2 ppm were assigned to the Cγ-Hγ in γ-acetylated *β*-O-4′ substructures (A′/A″), indicating that the *β*-O-4′ structure of the soluble lignin obtained from PHL underwent an acetylation reaction at the γ position. The signals of the methoxy groups and *β*-O-4′ substructures (substructure A) were the most prominent ones in both soluble and dioxane lignins. The signals corresponding to spirodienone (*β*-1′) substructures (D) could also be confirmed in the spectra of the soluble lignin, its C_β-H_β correlation being at δC/δH 61.1/3.2 ppm, and the schematic is shown in Fig. 3D. In the aromatic region, the signals of C_2-H_2 in guaiacyl units (G) were found at δC/δH 110/6.7 ppm in both soluble and dioxane lignin, suggesting that both soluble and dioxane lignins possessed a G-type structural unit, which is in agreement with the results of FTIR spectroscopy. Additionally, the signals at δC/δH

123.0/7.5 ppm were assigned to C_6-H_6 in ferulic acid ester, indicating that there was a ferulic acid ester structure in the soluble lignin from PHL.

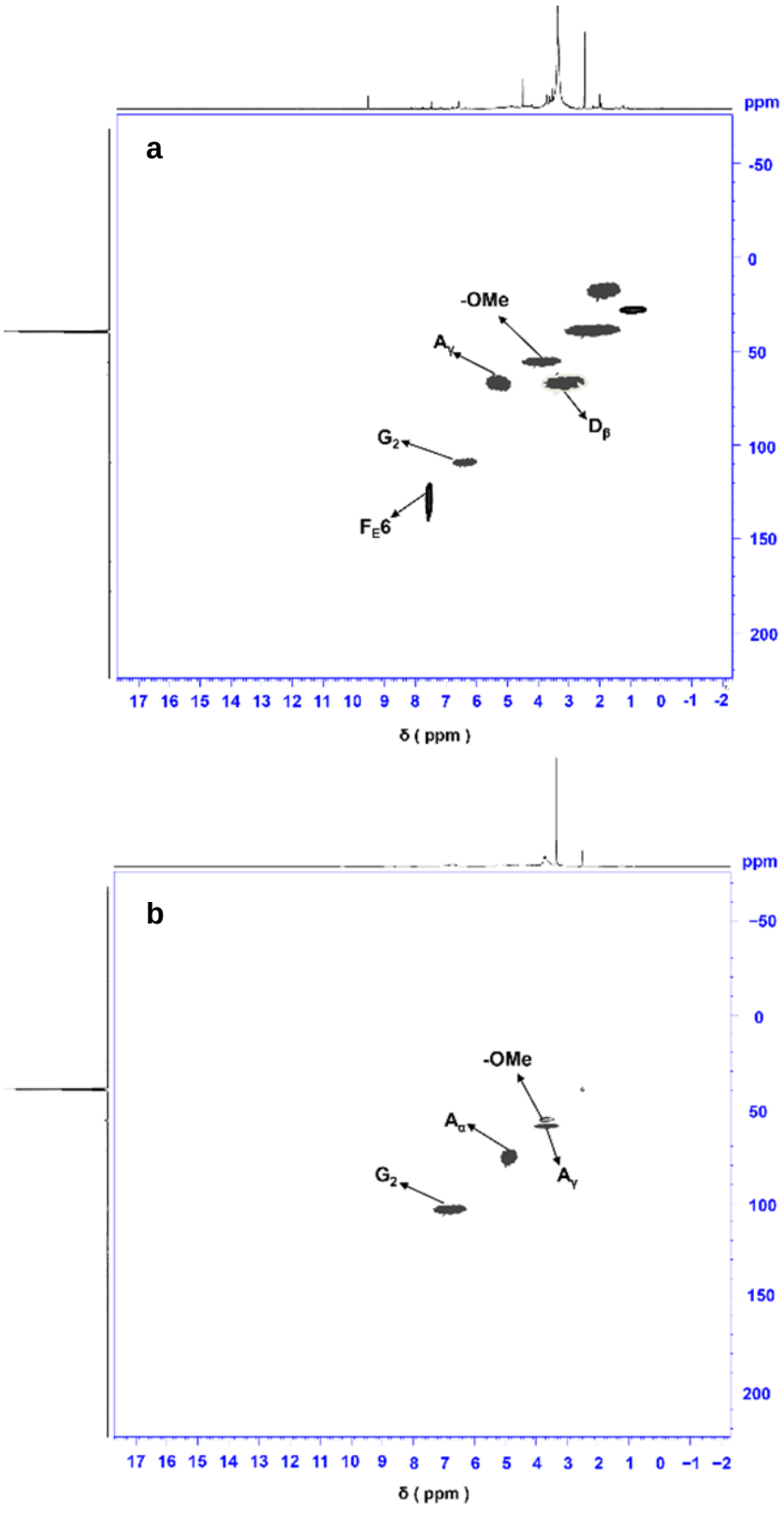

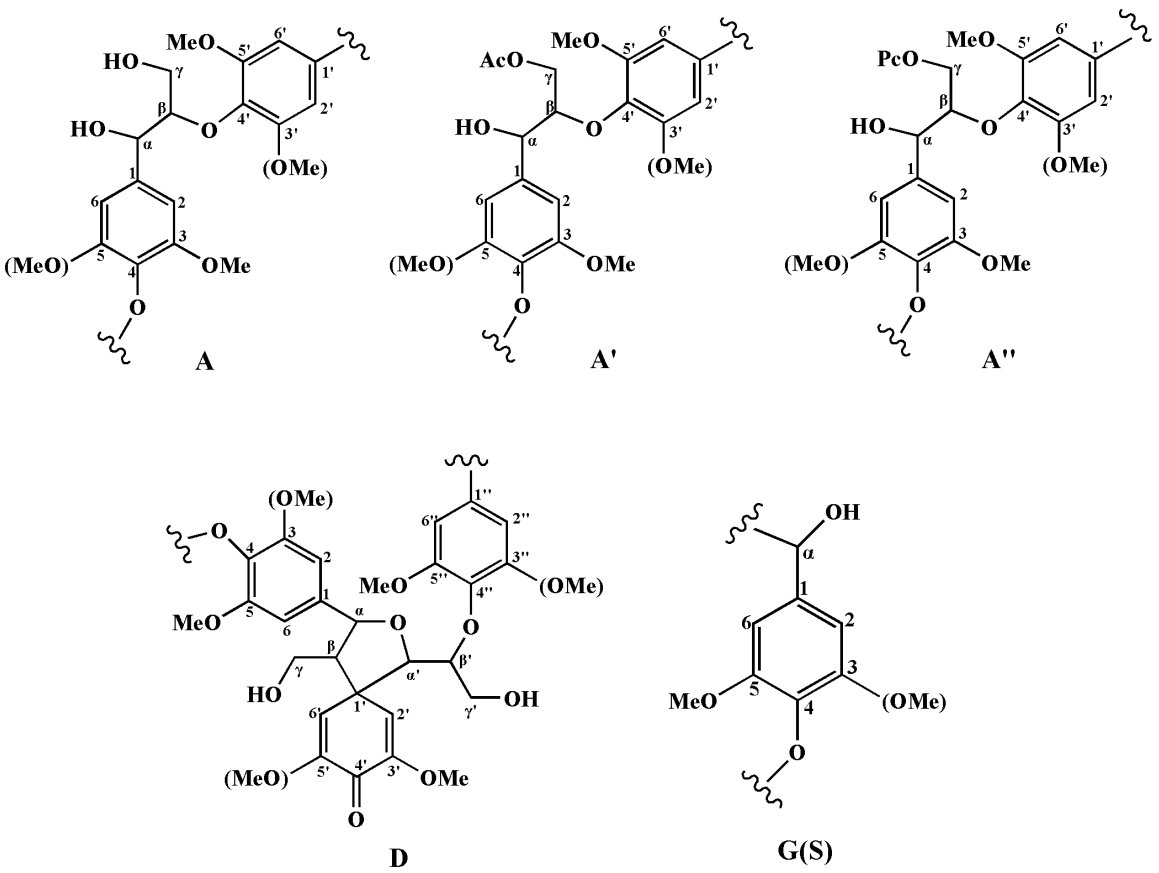

Fig. 3. 2D-HSQC spectra of the soluble (a); and dioxane (b) lignins. The lignin substructures are also shown: (A) *β*-O-4′ linkages; (A′, A") *β*-O-4′ linkages with acetylated γ-carbon; (D) C-H coupling structure of spiro structure; and (G(S)) guaiacyl unit or syringyl unit

Table 3. Assignments of Signals in the 2D-HSQC Spectra of Soluble and Dioxane Lignin

Label	δ_C/δ_H (ppm)	Assignments
-OMe	56.0/3.76	C-H in methoxyls
$A'_\gamma(A''_\gamma)$	63.5/4.2	Cγ-Hγ in γ-acetylated *β*-O-4′ substructures (A′/A″)
$A_{\alpha(S)}$	4.85/72.0	C_α-H_α in *β*-O-4′ substructures linked to a S unit (A)
D_β	61.1/3.2	C_β—H_β in *β*-1′ (spirodienone) substructures (D)
G_2	110/6.7	C_2-H_2 in guaiacyl (G)
F_E6	123.0/7.5	C_6-H_6 in Ferulic acid ester

Thermogravimetric Analysis

The thermal stability is a vital parameter for thermosetting or thermoplastic materials. Figure 4 shows the TG and derivative TG (DTG) curves of the soluble lignin obtained from PHL and dioxane lignin. The obtained soluble lignin sample had a maximum mass loss peak at 200 °C, which indicated the temperature at which hemicellulose begins to decompose was at approximately 200 °C. The maximum thermal decomposition of

lignin was observed at 350 °C to 450 °C (Liu 2009), consequently, hemicellulose has completed most of the decomposition when lignin begins to decompose. It can be seen that the maximum mass loss rate at 200 °C was caused by the decomposition of hemicellulose, which was due to the hemicellulose contained in the soluble lignin sample obtained by the activated carbon adsorption method.

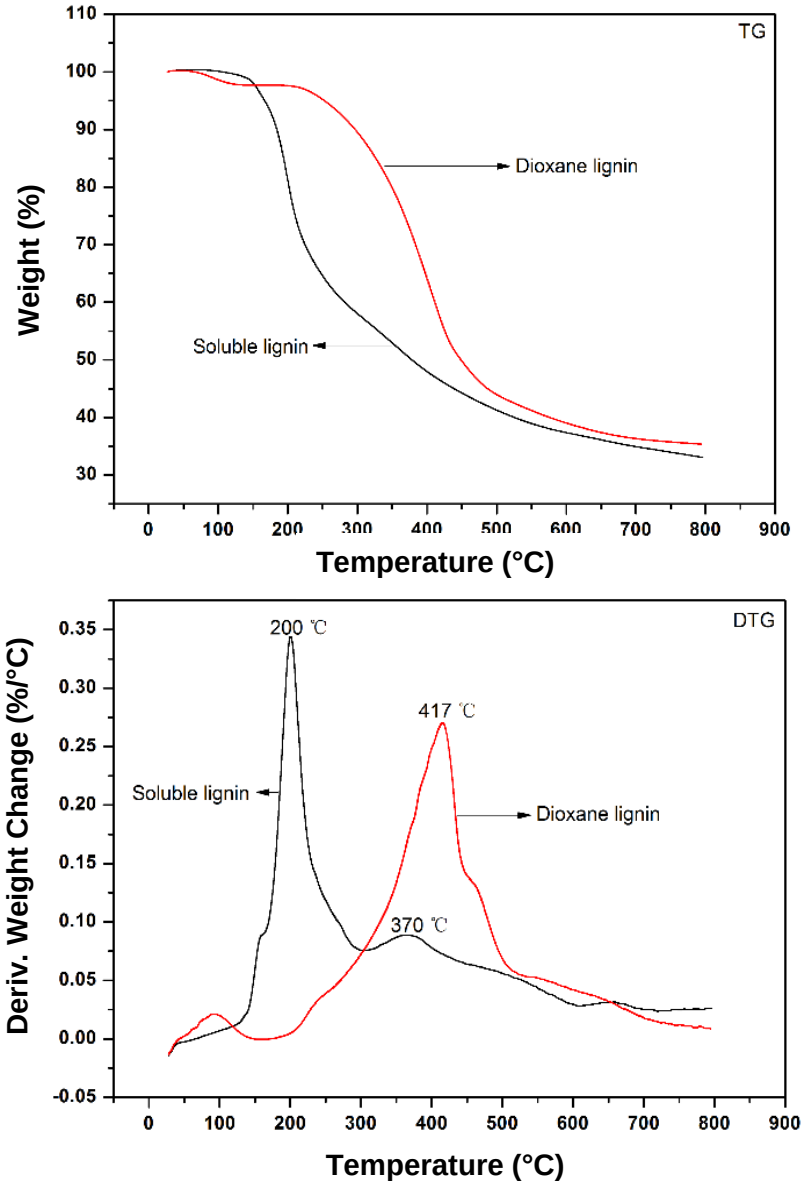

Fig. 4. TG/DTG curves of the soluble and dioxane lignins

The maximum thermal decomposition rate temperatures of soluble and dioxane lignins were at 370 °C and 417 °C, respectively. Previous literature also reported that the aromatic ring of lignin molecules began to disintegrate at temperatures above 400 °C (Sun *et al*. 2001). Above 500 °C, the mass loss and mass loss rate of soluble lignin and dioxane lignin basically converge. The residual char yields determined at 800 °C of soluble and dioxane lignins were 33.36% and 35.30%, respectively. Approximately 2% of yield gap between the two samples can be ascribed to the existence of hemicellulose component in

the obtained soluble lignin from PHL. Notably, the residual char yields of the two samples turned out to be almost the same, which exactly indicated that the main component of the sample obtained from PHL by activated carbon adsorption was lignin. Therefore, the soluble lignin obtained from PHL possessed thermal stability comparable to dioxane lignin, and the mixture of lignin and hemicelluloses can be used to produce carbon fiber by a combination process of electrospinning, carbonization and activation.

CONCLUSIONS

1. The present study compared the structural characteristics of soluble lignin in the PHL and dioxane-extracted lignin from bamboo-willow dissolving pulp. Results showed that the cleavage of *β*-O-4 aryl-ether linkages and demethylation occurred in the lignin structure during the pre-hydrolysis step.
2. The soluble lignin isolated from PHL could be identified as *p*-hydroxyphenyl-syringyl-guaiacyl (HSG) lignin, and the main linker bonds between structural units of soluble lignin were *β*-*β*, *β*-5, *β*-1, and *β*-O-4.
3. The soluble lignin obtained from PHL possessed thermal stability comparable to dioxane lignin from bamboo-willow material. This study will hopefully provide some guidance for the resource utilization and selective removal of soluble lignin in the PHL.

ACKNOWLEDGMENTS

The authors gratefully acknowledge the financial support from the National Science Foundation of Shandong Province (No. ZR2017LC016), the Open Fund of National Key Laboratory of Pulp and Paper Engineering, and the South China University of Technology (201817). The authors also appreciate the financial support from a project of Shandong Province Higher Educational Science and Technology Program (No. J17KA142) and the National Key R&D Program of China (2017YFB0307900).

REFERENCES CITED

Bardet, M., Robert, D., and Lundquist, K. (1985). "On the reactions and degradation of the lignin during steam hydrolysis of aspen wood," *Svensk Papperstidning* 88(6), r61-r67.

Buta, J. G., Zadrazil, F., and Galletti, G. C. (1989). "FT-IR determination of lignin degradation in wheat straw by white rot fungus *Stropharia rugosoannulata* with different oxygen concentrations," *Journal of Agricultural and Food Chemistry* 37(5), 1382-1384. DOI: 10.1021/jf00089a038

Capanema, E. A., Balakshin, M. Y., and Kadla, J. F. (2005). "Quantitative characterization of a hardwood milled wood lignin by nuclear magnetic resonance spectroscopy," *Journal of Agricultural and Food Chemistry* 53(25), 9639-9649. DOI: 10.1021/jf0515330

Chen, X., Cao, X., Sun, S., Yuan, T., Wang, S., Shi, Q., and Sun, R. (2019). "Hydrothermal acid hydrolysis for highly efficient separation of lignin and xylose

from pre-hydrolysis liquor of kraft pulping process," *Separation and Purification Technology* 209, 741-747. DOI: 10.1016/j.seppur.2018.09.032

Chua, M. G. S., and Wayman, M. (1979). "Characterization of autohydrolysis aspen (*P. tremuloides*) lignins. Part 3: Infrared and ultraviolet studies of extracted autohydrolysis lignin," *Canadian Journal of Chemistry* 57(19), 2603-2611. DOI: 10.1139/v79-421

Constant, S., Basset, C., Dumas, C., Di Renzo, F., Robitzer, M., Barakat, A., and Quignard, F. (2015). "Reactive organosolv lignin extraction from wheat straw: Influence of Lewis acid catalysts on structural and chemical properties of lignins," *Industrial Crops and Products* 65, 180-189. DOI: 10.1016/j.indcrop.2014.12.009

Del Rio, J. C., Rencoret, J., Marques, G., Li, J., Gellerstedt, G., Jimenez-Barbero, J., Martinez, A. T., and Gutierrez, A. (2009). "Structural characterization of the lignin from jute (*Corchorus capsularis*) fibers," *Journal of Agricultural and Food Chemistry* 57(21), 10271-10281. DOI: 10.1021/jf900815x

Evtuguin, D. V., Neto, C. P., Silva, A. M. S., Domingues, P. M., Amado, F. M. L., Robert, D., and Faix, O. (2001). "Comprehensive study on the chemical structure of dioxane lignin from plantation *Eucalyptus globulus* wood," *Journal of Agricultural and Food Chemistry* 49(9), 4252-4261. DOI: 10.1021/jf010315d

Ibrahim, M. M., Agblevor, F. A., and El-Zawawy, W. K. (2010). "Isolation and characterization of cellulose and lignin from steam-exploded lignocellulosic biomass," *BioResources* 5(1), 397-418. DOI: 10.15376/biores.5.1.397-418

Jahan, M. S., Liu, Z., Wang, H., Saeed, A., and Ni, Y. (2012). "Isolation and characterization of lignin from prehydrolysis liquor of kraft-based dissolving pulp production," *Cellulose Chemistry and Technology* 46(3-4), 261-667.

Jahan, M. S., and Mun, S. P. (2007). "Characteristics of dioxane lignins isolated at different ages of nalita wood (*Trema orientalis*)," *Journal of Wood Chemistry and Technology* 27(2), 83-98. DOI: 10.1080/02773810701486865

Kang, S., Xiao, L., Meng, L., Zhang, X., and Sun, R. (2012). "Isolation and structural characterization of lignin from cotton stalk treated in an ammonia hydrothermal system," *International Journal of Molecular Sciences* 13(11), 15209-15226. DOI: 10.3390/ijms131115209

Kang, S.-M., and Zhou, J.-C. (2012). "The application of NMR in lignin structure research," *China Pulp and Paper* 31(10), 58-63.

Kumar, H., and Christopher, L. P. (2017). "Recent trends and developments in dissolving pulp production and application," *Cellulose* 24(6), 2347-2365. DOI: 10.1007/s10570-017-1285-y

Lee, H. -J., Lim, W. -S., and Lee, J. -W. (2013). "Improvement of ethanol fermentation from lignocellulosic hydrolysates by the removal of inhibitors." *Journal of Industrial and Engineering Chemistry* 19(6), 2010-2015. DOI: 10.1016/j.jiec.2013.03.014

Leschinsky, M., Zuckerstätter, G., Weber, H. K., Patt, R., and Sixta, H. (2008). "Effect of autohydrolysis of *Eucalyptus globulus* wood on lignin structure. Part 1: Comparison of different lignin fractions formed during water prehydrolysis," *Holzforschung* 62(6), 645-652. DOI: 10.1515/hf.2008.117

Liu, Q. (2009). *Biomass Pyrolysis Mechanism Based on the Multi-components*, Ph.D. Dissertation, Zhejiang University, Zhejiang, China.

Lora, J. H., and Wayman, M. (1980). "Autohydrolysis of aspen milled wood lignin," *Canadian Journal of Chemistry* 58(7), 669-676. DOI: 10.1139/v80-102

Mašura, M. (1987). "Prehydrolysis of beechwood," *Wood Science and Technology* 21(1), 89-100. DOI: 10.1007/BF00349720

Schorr, D., Diouf, P. N., and Stevanovic, T. (2014). "Evaluation of industrial lignins for biocomposites production," *Industrial Crops and Products* 52(12), 65-73. DOI: 10.1016/j.indcrop.2013.10.014

Shen, J., Fatehi, P., Soleimani, P., and Ni, Y. (2011). "Recovery of lignocelluloses from pre-hydrolysis liquor in the lime kiln of kraft-based dissolving pulp production process by adsorption to lime mud," *Bioresource Technology* 102(21), 10035-10039. DOI: 10.1016/j.biortech.2011.08.058

Shen, J., Kaur, I., Baktash, M. M., He, Z., and Ni, Y. (2013). "A combined process of activated carbon adsorption, ion exchange resin treatment and membrane concentration for recovery of dissolved organics in pre-hydrolysis liquor of the kraft-based dissolving pulp production process," *Bioresource Technology* 127, 59-65. DOI: 10.1016/j.biortech.2012.10.031

Sluiter, A., Hames, B., Ruiz, R., Scarlata, C., Sluiter, J., and Templeton, D. (2006). *Determination of Sugars, Byproducts, and Degradation Products in Liquid Fraction Process Samples*, U. S. National Renewable Energy Laboratory, Golden, CO, USA.

Sun, R., Lu, Q., and Sun, X. F. (2001). "Physico-chemical and thermal characterization of lignins from *Caligonum monogoliacum* and *Tamarix* spp.," *Polymer Degradation and Stability* 72(2), 229-238. DOI: 10.1016/S0141-3910(01)00023-4

Tong, R. (2017). *Study on Lignin Removal Mechanism in Pre-hydrolysis Liquor of the Dissolving Pulp from Bamboo*, Master's Thesis, Qilu University of Technology, Shandong, China.

Tong, R., Wu, C., Zhao, C., and Yu, D. (2017). "Separation and structural characteristics of lignin in the prehydrolysis liquor of whangee dissolving pulp," *BioResources* 12(4), 8217-8229. DOI: 10.15376/biores.12.4.8217-8229

Wang, Q., Jahan, M. S., Liu, S., Miao, Q., and Ni, Y. (2014a). "Lignin removal enhancement from prehydrolysis liquor of kraft-based dissolving pulp production by laccase-induced polymerization," *Bioresource Technology* 164, 380-385. DOI: 10.1016/j.biortech.2014.05.005

Wang, Z., Jiang, J., Wang, X., Fu, Y., Li, Z., Zhang, F., and Qin, M. (2014b). "Selective removal of phenolic lignin derivatives enables sugars recovery from wood prehydrolysis liquor with remarkable yield," *Bioresource Technology* 174, 198-203. DOI: 10.1016/j.biortech.2014.10.025

Xiao, L. -P., Shi, Z. -J., Xu, F., and Sun, R. -C. (2012). "Characterization of MWLs from *Tamarix ramosissima* isolated before and after hydrothermal treatment by spectroscopical and wet chemical methods," *Holzforschung* 66(3), 285-302. DOI: 10.1515/hf.2011.154

Yang, G., Jahan, M. S., Ahsan, L., Zheng, L., and Ni, Y. (2013a). "Recovery of acetic acid from pre-hydrolysis liquor of hardwood kraft-based dissolving pulp production process by reactive extraction with triisooctylamine," *Bioresource Technology* 138, 253-258. DOI: 10.1016/j.biortech.2013.03.164

Yang, G., Jahan, M. S., and Ni, Y. (2013b). "Structural characterization of pre-hydrolysis liquor lignin and its comparison with other technical lignins," *Current Organic Chemistry* 17(15), 1589-1595. DOI: 10.2174/13852728113179990068

Zhang, J. -C., Wu, C. -J., and Yu, D. -M. (2019). "Effect of phosphoric acid in the pre-hydrolysis process of dissolving pulp production from bamboo-willow," *BioResources* 14(2), 3117-3131. DOI: 10.15376/biores.14.2.3117-3131

Zhao, J., Xiuwen, W., Hu, J., Liu, Q., Shen, D., and Xiao, R. (2014). "Thermal degradation of softwood lignin and hardwood lignin by TG-FTIR and Py-GC/MS," *Polymer Degradation and Stability* 108, 133-138. DOI: 10.1016/j.polymdegradstab.2014.06.006

Article submitted: September 3, 2019; Peer review completed: November 17, 2019; Revised version received and accepted: December 9, 2019; Published: December 11, 2019.
DOI: 10.15376/biores.15.1.825-839